ARTICLE IN PRESS

Available online at www.sciencedirect.com

SCIENCE DIRECT®

ELSEVIER

International Journal of Impact Engineering ▮ (▮▮▮▮) ▮▮▮–▮▮▮

INTERNATIONAL JOURNAL OF IMPACT ENGINEERING

www.elsevier.com/locate/ijimpeng

Time distance diagram of the jet initation of covered high explosive charges

M. Held*

TDW/EADS 86523 Schrobenhausen, Germany

Received 22 August 2005; received in revised form 23 February 2006; accepted 4 March 2006

Abstract

The bulging behaviour of a steel barrier in front and in contact with a high explosive charge desensitises the charge sensitivity for a shaped charge jet impact. The reasons are rampwave behaviour and pre-compression of the charge, which is explained in detail with a time distance diagram.

Keywords: Shaped charge jets; Initiation of high explosives; Covered charges; Bulging

1. Introduction

High explosive charges behave less sensitively in shaped charge jet initiation tests if the high explosive charge is in direct contact with a steel cover plate, in contrast to an air gap arrangement [1,2]. The built-up distances, the time delays Δt and the initiation times t_i, where for the initiation time t_i the detonation time t_D from the charge axis to the radial surface with $r = 24$ mm is subtracted from the delay time Δt ($t_i = \Delta t - 24\,\text{mm}/7.8\,\text{mm}/\mu\text{s}$), are shown as a function of jet impact velocity on the front surface of the acceptor charge for the charge with 10 mm air gap between barrier and the high explosive charge in Fig. 1 and in direct contact in Fig. 2. The initiation limit is 150–175 mm barrier thickness, respectively, in 3.2–3.0 mm/μs jet impact velocities in the case of an air gap and 75–100 mm barrier thickness, respectively, 4.8–4.2 mm/μs jet impact velocity in case of direct contact. The reason for this phenomenon is, after the author's opinion [2], the bulging behaviour of the steel barrier and the pre-compression of the high explosive charge, because also a 0.5 mm air gap between the barrier and the high explosive charge is desensitising the high explosive charge and gives similar build-up distances and delay time [3–5]. For this behaviour Chick and Hatt [6] and Frey et al. [7] have given a similar explanation. Frey specifically discussed ramp waves forming in the barrier and the fact that ramp waves are not effective agents for causing initiation. When thick barriers are present in contact with the high explosive charge, initiation occurs at the point, where a quasi-steady bow shock is formed in the explosive. But the bulging behaviour during jet penetration and perforation of the rear surface of a steel barrier is explained differently in the following paper in detail in terms of a time distance diagram.

*Tel.: +49 8252 996 345; fax: +49 8252 996 126.
E-mail address: Manfred.Held@EADS.com.

0734-743X/$ - see front matter © 2006 Elsevier Ltd. All rights reserved.
doi:10.1016/j.ijimpeng.2006.03.001

Nomenclature

P	depth
t	time
v	velocity
v_j	jet velocity
Z_0	distance to virtual origin
γ	$\sqrt{\rho_t/\rho_j}$
$\sqrt{\rho_t/\rho_j}$	target/jet density

Subscripts

st	for steel
HE	for high explosive

2. Time distance diagram

In the following time distance diagram, the bulging and the desensitisation behaviour of a steel barrier is quantitatively described. As a basic tool, a 44 mm shaped charge with wave shaper is used, which was and is

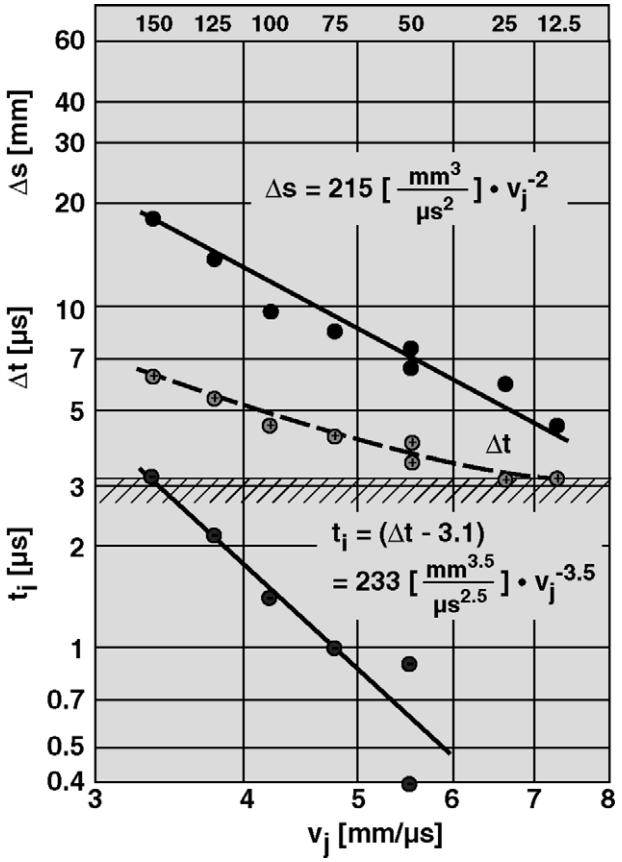

Fig. 1. Build-up distance Δs, delay times Δt and initiation times t_i as a function of jet impact velocities after different barrier thickness (top line), with the acceptor charge arranged at 15 mm air gap to the steel barrier rear surface.

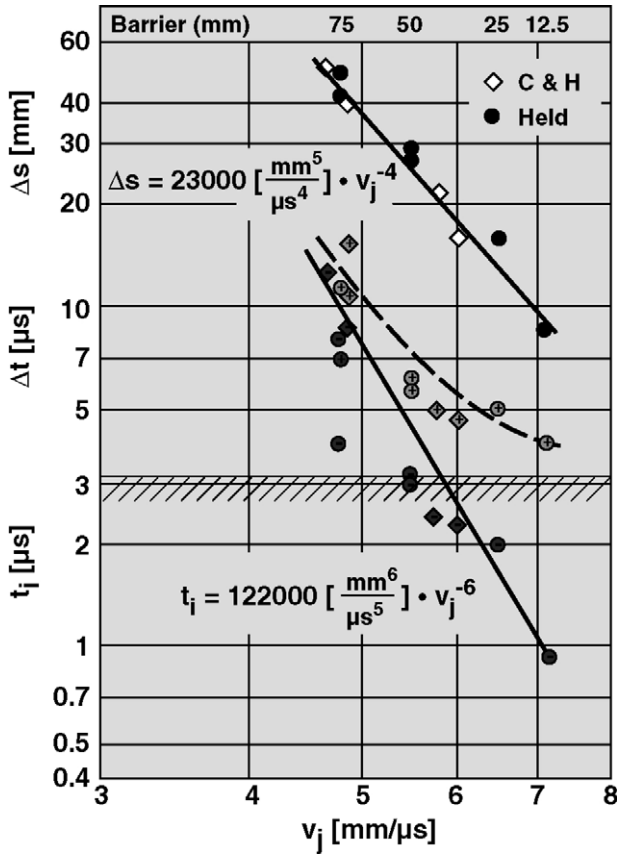

Fig. 2. Build-up distance Δs, delay times Δt and initiation times t_i as a function of jet impact velocities after different barrier thickness (top line), with the acceptor charge arranged at contact to the steel barrier.

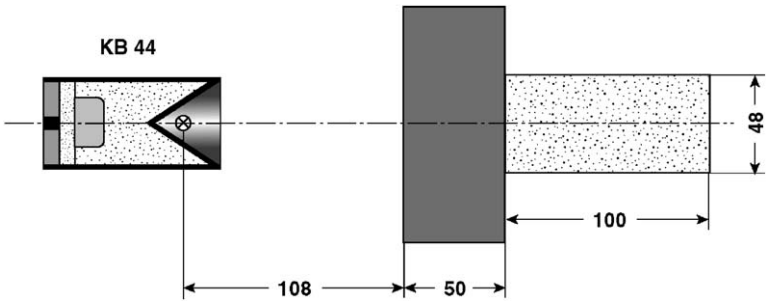

Fig. 3. Very often used test set—for the jet initiation studies by the author.

the typical test vehicle of the author for his jet initiation studies. The jet tip velocity is 8.3 mm/μs and the mean particulation time $t_P = 75$ μs. The zero point is selected on the front surface of a 50 mm thick steel barrier. The virtual origin Z_0 of the shaped charge has a distance of 108 mm to this steel barrier front surface (Fig. 3).

The so-called jet fan of the continuously stretching jet is drawn in the time distance diagram under the selected test set-up conditions (Fig. 4). These jet lines are calculated at two distances. One is the front surface of the barrier in 108 mm distance from the virtual origin, and the second is selected at the exit surface of the 50 mm thick steel barrier at 158 mm distance. To fit these data to the selected diagram, the calculated values have to be subtracted from the arrival time t_{j0} of the jet, which is 13.01 μs (108 mm/8.3 mm/μs). The calculated values for the jet fan are summarised in Table 1.

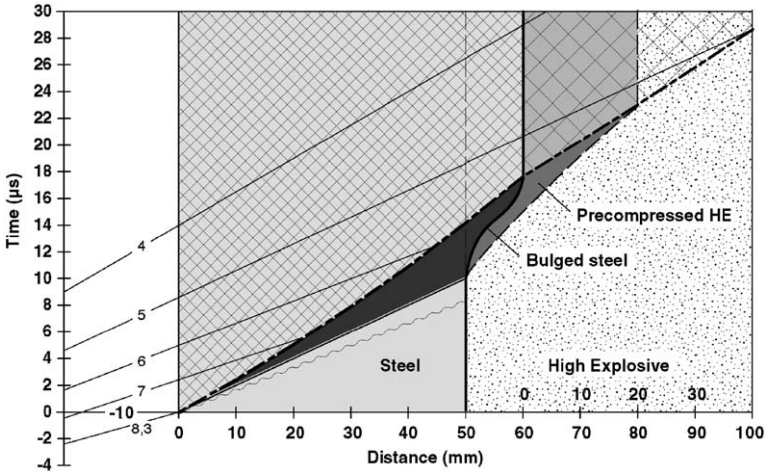

Fig. 4. Time distance diagram of a shaped charge jet, penetrating first a 50 mm thick steel barrier and then a pre-compressed attached high explosive charge.

Table 1
Jet fan data

v_j (mm/µs)	8.3	7	6	5	4
$108/v_j - 13.0$ (µs)	0	2.4	5	8.6	14
$158/v_j - 13.0$ (µs)	6	9.6	13.3	18.6	26.5

The continuously stretching jet penetrates the steel barrier. The penetration times t_{St} in the steel target as a function of penetration depth P can be calculated with Eq. (20) of reference [8].

$$t_{St} = (P + Z_0)^{(1+\gamma)} \cdot Z_0^{-\gamma} \cdot v_{j0}^{-1}, \tag{1}$$

where Z_0 is the distance of the front surface of the steel barrier to the virtual origin and γ is the square root of target to jet density:

$$\gamma = \sqrt{\rho_t/\rho_j}. \tag{2}$$

This γ value is for a steel target and a copper jet:

$$\gamma_{st} = \sqrt{7.85/8.9} = 0.939. \tag{3}$$

Introducing the values for Z_0 with 108 mm and γ with 0.939 the Eq. (1) can be transferred to

$$t_{st} = (P + 108)^{1.939} \times 108^{-0.939} \times 8.3^{-1}, \tag{4}$$

which gives

$$t_{st} = 1.483 \times 10^{-3}(P + 108)^{1.939}. \tag{5}$$

With this equation (5) the penetration times can be calculated as a function of crater depth, where again the arrival time t_{j0} (13 µs) of the jet tip has to be subtracted for the selected diagram, which starts with the front surface of the barrier with time zero.

It was assumed that a 50 mm thick steel barrier is bulging on the end surface with a value of about 10 mm, which gives a total penetration thickness of 60 mm for the jet, instead of the static 50 mm thickness. The residual jet velocity is decreasing by considering the bulging thickness for jet penetration. The residual jet velocities can be simply calculated over the total distance ($P + Z_0$) from the virtual origin and the total time

Table 2
Penetration times in the steel barrier

P (mm)	0	10	20	30	40	50	60
t_c (μs)	0	2.44	5.08	7.92	10.9	14.20	17.64

Table 3
Penetration times in the high explosive charge

P_{HE} (mm)	0	10	20	30	40	50
t_{HE} (μs)	17.64	20.30	23.02	25.80	28.65	31.56

$(\upsilon = (P + Z_0)/(t_c + t_0))$.

$$v_{j,50} = 158/(14.20 + 13.01) = 5.806\,\mathrm{mm}/\mu s, \tag{6}$$

$$v_{j,60} = 168/(17.64 + 13.01) = 5.481\,\mathrm{mm}/\mu s. \tag{7}$$

The simple consideration demonstrates that the residual jet velocity decreases with 0.325 mm/μs by the bulging steel barrier, which gives about a 6% difference (Table 2).

Then the exceeding jet with a residual jet velocity of 5.481 penetrates in the high explosive charge. The same Eq. (1), can be used but the γ-value for the high explosive charge, penetrated by a copper jet, has to be calculated to

$$\gamma_{HE} = \sqrt{1.7/8.9} = 0.437 \tag{8}$$

and the distance $Z_{0,HE}$ to the high explosive charge with 168 mm (108 + 50 + 10). This leads to the equation

$$t_{HE} = 0.0194(P + 168)^{1.437}. \tag{9}$$

Again, from this time t_{HE} the jet arrival time of 13.0 μs has to be subtracted to shift the times to the selected zero point in the given diagram. Table 3 gives these calculated values:

It was observed with a carefully arranged streak record of fine marks in a Plexiglass block that bulging of the barrier starts about 4–5 μs before the jet arrives on the end surface. Therefore the bulging starts at 10 μs which corresponds to 4.2 μs before the jet arrives at the 50 mm thick barrier rear surface at 14.20 μs (Table 2). This is a rough consideration. This test has shown that the high explosive charge is slowly loaded with a ramp wave, if the charge is in contact to the barrier, where it is promptly loaded by the impact at a free flying jet in the case of a large enough air gap.

Further the bulging steel barrier pre-compresses strongly the high explosive charge. The hot spots are squeezed out. In this diagram the pre-compression of the high explosive charge is drawn up to a distance of 30 mm behind the original barrier rear surface. In this dynamic case, the high explosive charge is additionally 20 mm compressed due to the bulging steel rear front. The jet with a residual velocity of 5.481 mm/μs is now first entering the compressed high explosive charge and approximately with the same value in the uncompressed high explosive charge in a distance of 30 mm to the original rear surface. This means that a build-up distance of around 30 mm is achieved before the jet is penetrating a non compressed high explosive charge. Initiation starts promptly when the jet reaches explosive material that has not been pre-compressed. The measured values were 26.8 and 29.4 mm in two earlier tests with 50 mm barrier thickness (see Fig. 2 [2]).

In this diagram the first arrival time of a shock wave is shown, which starts at the impact of the jet on the steel barrier front surface. The longitudinal sound velocity in steel is 5.95 mm/μs, which means the first shock waves are arriving after 8.4 μs on the steel barrier rear surface. After the different results of the author, these shock waves alone should not or at least very slightly influence the reaction behaviour of the high explosive charge.

3. Summary

A time distance diagram describes the jet perforation of a barrier in front of a high explosive charge. The jet tip arrives on the barrier front surface at time zero. It penetrates the steel barrier, where the jet is partially consumed from the tip on. It arrives after a time difference of 14.2 μs on the rear surface of a 50 mm thick barrier. But in front of the penetrating jet the steel material is moving and therefore bulging on the endsurface. The assumed bulging height is around 10 mm. Therefore, the jet arrives after the 60 mm dynamically bulged thick barrier in a time difference of 17.64 μs and has a residual jet tip velocity of 5.481 mm/μs. The jet further penetrates the pre-compressed high explosive charge. As soon as the jet enters the not strongly or not at all pre-compressed high explosive charge, the initiation of the high explosive charge starts.

The time distance diagram of a bulging material explains very well the less sensitive behaviour of high explosive charges in contact with steel barriers compared to charges with a large enough air gap distance to the barrier. The pre-compression also explains the larger build-up distances and longer delay or initiation times of the high explosive charges under such test arrangements compared to charges which are not in direct contact with a steel barrier.

References

[1] Chick MC, Hatt DJ. The Initiation of covered composition B by a metal jet. Propell Explos Pyrotech 1983;8:121–6.
[2] Held M. Initiation phenomena with shaped charge jets.In: Ninth international symposium on detonation. 1989. p.1.416–1.426; 1432–1440.
[3] Held M. Experiments of initiation of covered but unconfined high explosive charges by means of shaped charge jets. Propell Explo Pyrotec 1987;12:35–40.
[4] Held M. Experiments of initiation of covered but unconfined high explosive charges under different test conditions by shaped charge jets. Propell Explos Pyrotec 1987;12:97–100.
[5] Held M. Discussion of the experimental findings from the initiation of covered but unconfined high explosive charges with shaped charge jets. Propell Explos Pyrotech 1987;12:167–74.
[6] Chick M, Hatt DJ, Mac Intyre ID, Frey RB. The jet initiation of solid explosives. In: Eighth international symposium on detonation, 1985; p. 318–327.
[7] Frey B, Lawrence W, Chick M. Shock evolution after shaped charge jet impact and its relevance to explosive initiation. Int J Impact Eng 1995;16(4):563–70.
[8] Held M. Hydrodynamic theory of shaped charge jet penetrations. J Explos Propell R O C—Taiwan 1991;7:9–24.